DOI: 10.1093/jnci/djr451
Advance Access publication on October 31, 2011.

ARTICLE

Differentiation Therapy: Targeting Human Renal Cancer Stem Cells with Interleukin 15

Sandy Azzi, Stefania Bruno, Julien Giron-Michel, Denis Clay, Aurore Devocelle, Michela Croce, Silvano Ferrini, Salem Chouaib, Aimé Vazquez, Bernard Charpentier, Giovanni Camussi, Bruno Azzarone, Pierre Eid

Manuscript received February 28, 2011; revised September 16, 2011; accepted September 30, 2011.

Correspondence to: Pierre Eid, PhD, and Bruno Azzarone, MD, PhD, INSERM UMR 1014, Lavoisier Building, Paul Brousse Hospital, 94807 Villejuif, France (e-mail: pierre.eid@inserm.fr; bazzarone@hotmail.com).

Background Many renal cancer patients experience disease recurrence after immunotherapy or combined treatments due to persistence of cancer stem cells (CSCs). The identification of reliable inducers of CSC differentiation may facilitate the development of efficient strategies for eliminating CSCs. We investigated whether interleukin 15 (IL-15), a regulator of kidney homeostasis, induces the differentiation of CD105-positive ($CD105^+$) CSCs from human renal cancers.

Methods $CD105^+$ CSCs were cultured to preserve their stem cell properties and treated with recombinant human IL-15 (rhIL-15) to evaluate their ability to differentiate, to acquire sensitivity to chemotherapeutic drugs, and to form spheroids in vitro and tumors in vivo. Expression of stem cell and epithelial markers were studied by flow cytometry, immunocytochemistry, and immunoblotting. Identification of a CSC side population fraction and its sensitivity to chemotherapy drugs and expression of ATP-binding cassette (ABC) transporters and aldehyde dehydrogenase (ALDH) activities were determined by flow cytometry. Spheroid formation was determined in limiting dilution assay. Xenograft tumors were generated in severe combined immunodeficient mice (n = 12–18 mice per group). All statistical tests were two-sided.

Results $CD105^+$ CSCs treated with rhIL-15 at 10 pg/mL differentiated into cells expressing epithelial markers. rhIL-15 induced epithelial differentiation of all $CD105^+$ CSCs subsets and blocked CSC self-renewal (sphere-forming ability) and their tumorigenic properties in severe combined immunodeficient mice. Vinblastine and paclitaxel induced statistically significant higher levels of apoptosis in rhIL-15-differentiated epithelial cells compared with $CD105^+$ CSCs (mean percentage of apoptotic cells, vinblastine: 33% vs 16.5%, difference = 16.5%, 95% confidence interval = 12.25% to 20.74%, $P = .0025$; paclitaxel: 35% vs 11.6%, difference = 23.4%, 95% confidence interval = 22.5% to 24.24%, $P = .0015$). The higher sensitivity of rhIL-15-differentiated epithelial cells to chemotherapeutic drugs was associated with loss of detoxifying mechanisms such as ALDH and ABC transporter activities.

Conclusion IL-15 directs the epithelial differentiation of renal CSCs and meets the criteria for a treatment strategy: CSC pool depletion and generation of differentiated nontumorigenic cells that are sensitive to chemotherapeutic agents.

J Natl Cancer Inst 2011;103:1884–1898

Despite the clonal origin of many cancers, leukemia and some solid cancers, including renal cell carcinoma, appear to be heterogeneous in terms of tumor cell proliferation and differentiation. Most tumor cells are destined to differentiate and will eventually stop dividing. However, in the bulk of acute myeloid leukemia and in many solid tumors, the existence of a small minority of cancer cells displaying stem cell–like features has been demonstrated (1–5). These cells were identified as cancer stem cells (CSCs) or cancer-initiating cells based on their capacity for self-renewal and to recapitulate tumor pathophysiology in an immunocompromised animal model (6,7). The CSCs share several properties in common with normal stem cells and have been identified and isolated on the basis of their expression of specific combinations of molecules (eg, CD133, CD44, ATP-binding cassette proteins [ABC transporter proteins], aldehyde dehydrogenase [ALDH]) (5,8). Moreover, CSCs are more resistant to conventional chemotherapy compared with more differentiated cancer cells (5). The chemoresistance of CSCs reflects their quiescent nature and their high capacity for DNA repair, high levels of anti-apoptotic proteins, and use of multiple mechanisms for inactivating or eliminating cytotoxic drugs (9). The inherent drug resistance and strong tumorigenic and metastatic properties of CSCs (5,8) may explain why many cancer patients, particularly those with solid tumors, do not respond to cancer treatments (including chemotherapy, radiotherapy, and tumor-targeted agents) and the rapidity of relapse after initial remission. Current anticancer treatments that fail to

kill CSCs nonetheless shrink primary and metastatic tumors; however, these effects are often transient, and relapses of most metastatic cancers frequently occur. Efforts to cure cancer must therefore include treatments that target CSCs as well as proliferating cells. Potential approaches to killing CSCs include blocking self-renewal signaling, inhibiting cell survival mechanisms, and inducing tumor cell differentiation (9–11).

The above-mentioned approaches are relevant in renal clear cell carcinoma (RCC), which is highly chemo- and radioresistant (12) and where a rare subset of CSCs that express the mesenchymal stem cell marker CD105 and display properties of stem cells, such as clonogenicity and expression of the stem cell markers Nestin, Nanog, and Oct-3/4, has been isolated (6). These CD105-positive ($CD105^+$) CSCs lack markers of epithelial differentiation and can differentiate into either epithelial or endothelial cells and can generate serially transplantable tumors in immunocompromised mice (6). In this context, it is therefore important to understand the molecular mechanisms that regulate stem cell properties to develop efficient strategies aiming to eliminate and/or differentiate $CD105^+$ CSCs.

Thus, we examined the effects of treating $CD105^+$ CSCs with interleukin 15 (IL-15), which is not only a powerful immune stimulator (13) but also acts on non-immunocompetent cells by controlling neuronal stem cell differentiation (14), playing important roles in renal homeostasis, acting through autocrine–paracrine loops as a survival factor (15), and preserving E-cadherin expression (J. Giron-Michel, S. Azzi, P. Eid, B. Azzarone, unpublished data). We therefore investigated whether this cytokine could modify the stem cell–like characteristics of human renal $CD105^+$ CSCs.

CONTEXT AND CAVEATS

Prior knowledge

The persistence of cancer stems cells (CSCs), which are inherently drug resistant and strongly tumorigenic, may explain why many renal cancer patients experience disease recurrence after immunotherapy or combined treatments. Effective treatments must therefore target CSCs as well as proliferating cells. One approach is to induce differentiation of CSCs into nontumorigenic epithelial cells.

Study design

In vitro assays and a mouse model were used to examine the effects of interleukin 15 (IL-15) on the stem cell–like characteristics and tumorigenicity of human renal CSCs that express the mesenchymal stem cell marker CD105 ($CD105^+$ CSCs).

Contribution

IL-15 induced the stable epithelial differentiation of renal $CD105^+$ CSCs, generating a differentiated nontumorigenic cell population that was more sensitive to cytotoxic drugs compared with the parental CSCs.

Implications

IL-15-mediated epithelial differentiation of renal cancer stem cells meets the criteria for major treatment strategies: depletion of the CSC pool and generation of differentiated nontumorigenic cells with increased sensitivity to chemotherapeutic agents.

Limitation

In vivo, some unknown microenvironmental parameters other than hypoxia (eg, cytokines, stromal cells) may limit the action of IL-15 inside CSC niches.

From the Editors

Materials and Methods

Antibodies, Cytokines, and Reagents

Antibodies against ERK (rabbit polyclonal, 1:250 dilution), IL-2Rβ (sc-1046 rabbit polyclonal, 1:250 dilution), IL-2Rγ (sc-670 rabbit polyclonal, 1:250 dilution), and villin (sc-58898 mouse monoclonal, 1:250 dilution) were obtained from Santa Cruz Biotechnology (Delaware, CA). Antibodies specific for phosphorylated ERK (rabbit polyclonal, 1:1000 dilution) and phosphorylated IκBα (mouse polyclonal, 1:1000 dilution) and the Alexa fluor–conjugated rabbit monoclonal antibody against phosphorylated STAT5 (1:500 dilution) were obtained from Cell Signaling (Beverly, MA). Antibodies against IL-15Rα (AF247 goat polyclonal, 1:1000 dilution), phosphorylated STAT5 (rabbit polyclonal, 1:1000 dilution), E-cadherin (AF648 goat polyclonal, 1:1000 dilution), Nanog (AF1997 goat polyclonal, 1:1000 dilution), Nanog–phycoerythrin conjugated (IC1997P goat polyclonal, 1:200 dilution), Oct-3/4 (AF1759 goat polyclonal, 1:1000 dilution), Oct-3/4–phycoerythrin conjugated (IC1759P goat polyclonal, 1:200 dilution), and Nestin–phycoerythrin conjugated (IC1259P mouse monoclonal, 1:200 dilution) were purchased from R&D Systems Europe Ltd (Abingdon, UK). Fluorescein isothiocyanate–conjugated anti-CD90 (mouse monoclonal, 1:100 dilution) was purchased from Dianova GmbH (Hamburg, Germany). The pan-cytokeratin antibody (pan-CK mouse monoclonal, 1:1000 dilution) was obtained from EXBIO (Prague, Czech Republic). Rhodamine-conjugated phalloidin (1:5000 dilution) for F-actin detection and a mouse monoclonal antibody against zonula occludens-1 (ZO-1, 1:1000 dilution) were obtained from Invitrogen (Cergy-Pontoise, France). The anti-β-actin monoclonal antibody (A1978, 1:2500 dilution), anti-glyceraldehyde 3-phosphate dehydrogenase rabbit monoclonal antibody (G9545, 1:5000 dilution), verapamil (cat. no. 381195), and Hoechst 33342 were obtained from Sigma-Aldrich (St Louis, MO). Horseradish peroxidase (HRP)–conjugated (1:5000 dilution) and fluorescent (1:200 dilution) secondary antibodies were purchased from Jackson ImmunoResearch (West Grove, PA). The neutralizing anti-IL-15 monoclonal antibody M111 (final concentration 10 μg/mL) was a gift from Dr Phalmer Christy (Amgen, Thousand Oaks, CA). The antibody against CD105 (MEM-229 mouse monoclonal, 1:200 dilution) and recombinant human IL-15 (rhIL-15) were obtained from ImmunoTools (Friesoythe, Germany).

Cell Culture

$CD105^+$ CSCs were identified and isolated from human renal carcinomas as previously described (6). Briefly, cell suspensions were obtained through collagenase II digestion of specimens of renal cell carcinomas. Aliquots of the cell suspension were subjected to fluorescence-activated cell sorting (FACS) analysis for quantification of $CD105^+$ cells, which were isolated by using an anti-CD105 antibody coupled to magnetic beads and a magnetic-activated cell sorting system (Miltenyi Biotec, Auburn, CA).

$CD105^+$ CSCs were cultured in a multipotent adult progenitor cell medium (complete low-glucose Dulbecco's modified Eagle medium [DMEM-LG]), which consisted of DMEM-LG (Invitrogen, Paisley, UK), supplemented with insulin–transferrin–selenium (Invitrogen, Paisley, UK), 10^{-9} M dexamethasone, 100 U penicillin, 1000 U streptomycin, 10 ng/mL epidermal growth factor (Sigma-Aldrich), and 5% fetal calf serum (FCS; EuroClone, Wetherby, UK). Adherent clones were maintained in complete DMEM-LG for more than 50 passages, with no change in the expression of stem cell markers as determined by FACS analysis. Primary normal human renal epithelial cells (RPTECs) derived from a noncancerous kidney (Lonza, Verviers, Belgium) were expanded in vitro according to the supplier's instructions. RPTECs were cultured in REGM Renal Epithelial Cell Growth medium (Lonza), which was changed daily to ensure the maintenance of epithelial characteristics. The human renal carcinoma samples were collected and handled in accordance with the Declaration of Helsinki. This study was approved by the Center for Molecular Biotechnology Institutional Review Board, University of Torino.

In Vitro Epithelial Cell Differentiation. In the first model of epithelial cell differentiation, $CD105^+$ CSCs in complete DMEM-LG were transferred to RPMI high-glucose medium (Invitrogen, Cergy-Pontoise, France) containing 10% FCS, without growth factors, for 3 weeks (6). Epithelial cells obtained after 3 weeks of RPMI culture are called RPMI-EP. In the second model of epithelial cell differentiation, $CD105^+$ CSCs were maintained in complete DMEM-LG that was supplemented with 10 pg/mL of rhIL-15 every 3 days for 4 weeks. Epithelial cells obtained by treatment of $CD105^+$ CSCs with rhIL-15 for 4 weeks are called rhIL-15-EP. In some experiments, we expanded rhIL-15-EP for an additional 2 weeks in complete DMEM-LG without rhIL-15. These 6-week-old cells are called rhIL-15-EP6w. The low concentration of rhIL-15 (10 pg/mL), which is sufficient to activate the high-affinity IL-15R (13), is slightly higher than the concentration of IL-15 in the sera of normal donors (ie, 6–7 pg/mL) (16) and equal to the amount of cytokine secreted by normal renal epithelial cells (10 pg/mL) (17). In some experiments, rhIL-15 was also used at a higher "supraphysiological" concentration not found in biological fluids (ie, 10 ng/mL) to activate the intermediate-affinity IL-15R (16).

Sphere Formation Assays. We evaluated the ability of $CD105^+$ CSCs and $CD105^+$ CSCs treated with rhIL-15 for 1 or 3 weeks to grow as floating spheres in nonadherent conditions by plating cells (1×10^3 cells per well) in serum-free complete DMEM-LG on ultralow attachment six-well plates (Fisher Scientific, Paris, France). Spheroid formation was evaluated under a light microscope after 1 week at 37°C. We also evaluated the self-renewal capacity of $CD105^+$ CSCs by performing a limiting dilution assay for spheroid formation. $CD105^+$ CSCs were plated using a FACS DiVa cell sorter equipped with autoclone software (Beckton Dickinson, Le Pont-de-Claix, France) at a density of one cell per well in ultralow attachment 96-well plates (Corning Life Sciences, Acton, MA). Each well was supplemented with 200 µL of serum-free complete DMEM-LG that contained or lacked 10 pg/mL of rhIL-15. After 3 weeks, each well was examined under a light microscope, and the total number of wells containing spheroid colonies was determined. Five replicates were used for each condition, and the experiment was repeated two times.

Flow Cytometry Analyses

For all assays described below, we acquired fluorescence data for 10 000 to 50 000 events on a FACSCalibur flow cytometer (BD Biosciences, Oxford, UK) and analyzed the data with the use of CellQuest software (BD Biosciences). Three replicates were used for each condition, and the experiment was repeated at least three times.

Expression of Cellular Antigens. Expression of cell surface (E-cadherin, CD105, IL-15R, Nestin) and intracellular (Oct-3/4, Pan-CK) antigens was analyzed by flow cytometry as previously described (6,18,19). Briefly, suspensions of enzymatically detached cells were permeabilized (for intracytoplasmic staining) or not (for cell surface staining) with BD Cytofix/Cytoperm reagent (BD Pharmingen, Le Pont-De-Claix, France), and 10^5 cells were suspended in RPMI medium supplemented with 1% FCS and stained with conjugated antibodies directed against the above mentioned cell markers at the dilutions indicated in the "Antibodies, Cytokines, and Reagents" section. Subsequently, cells were fixed by incubation with 1% paraformaldehyde in phosphate-buffered saline (PBS) for 20 minutes at room temperature and analyzed by flow cytometry.

ALDH detection. ALDH activity was assessed by flow cytometry in $CD105^+$ CSCs and their differentiated counterparts (rhIL-15-EP or RPMI-EP) with the use of an ALDEFLUOR kit (StemCell Technologies, Grenoble, France) in accordance with the manufacturer's instructions. Briefly, 10^6 $CD105^+$ CSCs, rhIL-15-EP, and RPMI-EP were incubated with BODIPY aminoacetaldehyde, which is converted into a fluorescent molecule (BODIPY aminoacetate) in the cytoplasm. Specificity of the fluorescent reaction was shown using the specific ALDH inhibitor diethylaminobenzaldehyde (DEAB).

Dye Efflux. To evaluate dye efflux activity, $CD105^+$ CSCs, rhIL-15-EP, and RPMI-EP were resuspended at a density of 10^6 cells per mL in RPMI-1640 medium supplemented with 1% FCS and incubated for 90 minutes at 37°C with 5 mg/mL Hoechst 33342 dye (B2261, bisBenzimide HOE 33342; Sigma-Aldrich) in the presence or absence of 50 µM verapamil, an inhibitor of ABC transporters. The cells were washed with 2% bovine serum albumin (BSA) in cold Hanks balanced salt solution to remove unincorporated dye. Subsequently, cells were resuspended in RPMI-1640 medium supplemented with 1% FCS and analyzed by flow cytometry for Hoechst 33342 dye intracellular staining. This standard flow cytometry assay is based on analysis of the wavelengths of blue and red light emission for double-stranded DNA labeled with the Hoechst 33342 marker, making it possible to distinguish between "G_0/G_1" and "$S/G_2/M$" cell populations. The efflux activity of each population is then determined (20). This method distinguishes a subpopulation of cells that originates from G_0/G_1 cells called the side population. The side population, which has a high dye efflux capacity, corresponds to the most primitive

CSCs, whereas the non–side population subset contains principally committed CSCs (20).

STAT5 Activation. We investigated STAT5 activation in the side population and non–side population subsets of $CD105^+$ CSCs by treating cells with 10 pg/mL of rhIL-15 during the last 45 minutes of staining with Hoechst 33342 dye. Treated and untreated cells were detached by trypsin, washed, and fixed by incubation with 1% paraformaldehyde in PBS for 20 minutes at room temperature. The cells were permeabilized by resuspension, with vortexing, in ice-cold methanol and incubated at 4°C for 10 minutes. The cells were washed in 1% BSA in PBS and incubated with an Alexa Fluor 488–conjugated mouse monoclonal antibody against phosphorylated STAT5 (Cell Signaling) for 60 minutes at 4°C. The cells were analyzed by gating on side population and non–side population subsets.

IL-15 Response Under Hypoxic Conditions. $CD105^+$ CSCs (5×10^5 cells in T25 flask) were cultured for 48 hours in normoxic conditions (ie, 20% O_2, 5% CO_2, and 75% N_2 at 37°C) and subsequently incubated for an additional 24 hours in an $InVivo_2$ 400 Hypoxia Workstation (Ruskinn, Bridgend, UK) under hypoxic conditions in a humidified atmosphere containing 5% CO_2, 1% O_2, and 94% N_2 at 37°C. The cells were treated for 45 minutes with rhIL-15 (10 pg/mL) and then harvested and fixed without reoxygenation for analysis of STAT5 phosphorylation as described above.

Cell Cycle Analysis. $CD105^+$ CSCs and $CD105^+$ CSC–derived cells at various stages of the epithelial differentiation process (ie, $CD105^+$ CSCs incubated for 1–4 weeks with rhIL-15 or for 3 weeks in RPMI) were treated with paclitaxel or vinblastine (0.1 μM each) for 24 hours, harvested, and fixed by overnight incubation with 95% ethanol at 4°C. The cells were incubated for 30 minutes with RNase A (50 μg/mL; Roche Applied Science, Indianapolis, IN), followed by incubation with propidium iodide (50 μg/mL) for 30 minutes at 37°C. Intracellular propidium iodide fluorescence intensity was then determined.

Enzyme-Linked Immunosorbent Assay (ELISA) of Secreted IL-15

To evaluate IL-15 secretion during $CD105^+$ CSC differentiation, cell supernatants were harvested weekly during the differentiation process, and the concentration of IL-15 in supernatants was determined in duplicate using enzyme-linked immunosorbent assay Quantikine D1500 (R&D systems). Supernatants of primary cultures of human RCCs prepared as previously described (18) and of RPTEC were used as negative and positive controls, respectively. Serial dilutions of a purified rhIL-15 preparation (stock solution of 2500 pg/mL) in Calibrator Diluent RD5-5 (R&D systems) were used to generate a standard curve that started at 0 pg/mL and ended at 250 pg/mL. Absorbance was read at 450 nm with the use of a Smart Spec 3000 microplate reader (Bio Rad, Hercules, CA).

Immunoblot Analyses

To evaluate IL-15R expression during $CD105^+$ CSC differentiation, total cell lysates were prepared and the α, β, and γ chains of IL-15R were analyzed by immunoblotting as previously described (19). For analysis of signal transduction, $CD105^+$ CSCs were serum starved overnight and treated with 10 pg/mL of rhIL-15 for 2–40 minutes. Activation was interrupted by adding two to three volumes of ice-cold PBS. The cells were harvested by centrifugation 5 minutes at 500*g*, and the cell pellets were lysed by incubation for 30 minutes on ice in 1% Triton X-100, 20 mM Tris–HCl (pH 7.4), 137 mM NaCl, 2 mM EDTA, 2 mM sodium pyrophosphate, and 10% glycerol in the presence of phosphatase inhibitors (25 mM β-glycerophosphate and 1 mM sodium orthovanadate) and complete protease inhibitor cocktail tablets (Roche Applied Science). The cell debris was removed by centrifugation (9000*g*), and the proteins in the supernatant were resolved by sodium dodecyl sulfate–polyacrylamide gel electrophoresis and transferred to a polyvinylidene fluoride membrane as previously described (18). Antibody binding was detected with the use of HRP-conjugated secondary antibodies (1:5000 dilution, Jackson Immunoresearch). HRP detection was performed with the use of an Immobilon Western kit (Millipore, Molsheim, France).

Immunocytochemistry

$CD105^+$ CSCs and rh-IL-15-EP6w were dispensed into an eight-well Lab-Tek tissue culture chamber slide (1×10^5 cells per well; Nunc, Naperville, IL), and antibody staining was performed when the cells reached confluence. For membrane staining (ie, with antibodies against E-cadherin, CD105, or nestin), the cells were fixed by incubation with cold methanol:acetone (1 vol:1 vol) for 10 minutes at −20°C, washed, and incubated for 60 minutes with 3% BSA in PBS to block nonspecific binding. For intracellular staining (ie, with α-actin, pan-cytokeratin, Oct-3/4, Nanog, villin, and vimentin antibodies), the cells were fixed with 4% (wt/vol) paraformaldehyde in PBS and permeabilized by incubation for 1 minute with 0.5% Triton X-100 in PBS. The cells were incubated with blocking solution (3% BSA in PBS) and incubated overnight at 4°C with the various antibodies. The cells were then washed and incubated with Alexa Fluor 488–conjugated rabbit anti-mouse or anti-goat IgG diluted in blocking solution and incubated for 30 minutes. F-actin organization was revealed staining the cells with 0.2 μg/mL of rhodamine-conjugated phalloidin for 20 minutes. The cells were washed with PBS, mounted in 4,6-diamidino-2-phenylindole (Invitrogen, Cergy-Pontoise, France), and visualized by fluorescence microscopy (Leica, Solms, Germany).

Measurement of Transepithelial Electrical Resistance

Polarized epithelial cells have a distinctive apical–basal axis of polarity for the vectorial transport of ions and solutes across the epithelium. Their closed epithelium enables them to regulate the exchange of nutrients and waste between the internal and external environments. These functions require a transepithelial osmotic gradient, which can be assessed in vitro by electrophysiological measurements of transepithelial electrical resistance across monolayers by use of the electrical cell impedance sensing technique (Applied Biophysics, Troy, NY). Therefore, transepithelial electrical resistance is widely used as an indicator of the epithelium integrity and of the degree of tight junctions organization between cells. $CD105^+$ CSCs, rhIL-15-EP, and RPMI-EP (10^5 cells per well) were plated in triplicate in Transwell plates containing collagen-coated polycarbonate filters (Corning Costar Corporation, Cambridge, UK) and cultured for 3 days, to confluence, in complete DMEM-LG or RPMI medium. We used

human tubular epithelial cells (RPTECs; Lonza) as a positive control. We used an EVOM epithelial volt-ohm meter (World Precision Instruments Inc, Sarasota, FL) to determine transepithelial electrical resistance, which was expressed in ohms × cm^2. High transepithelial electrical resistance levels (values over 500 ohms × cm^2) reflect regulated cellular transport processes in the epithelium, whereas a low transepithelial electrical resistance level (values below 200 ohms × cm^2) renders the epithelium leaky (21). Assays were performed in triplicate, and all results were normalized with respect to the area of the membrane. The experiment was performed three times.

MTT Analysis of Cell Proliferation

We used the tetrazolium salt 3-(4,5-dimethylthiazol-2-yl)-2,5-diphenyltetrazolium bromide (MTT) assay to assess the effects of chemotherapy drugs on cell proliferation in vitro. $CD105^+$ CSCs and derived cells at various stages of epithelial differentiation (ie, $CD105^+$ CSCs incubated for 1–4 weeks with rhIL-15 or for 3 weeks in RPMI) were plated in 96-well plates at a density of 1000 cells per well in 200 μL of medium per well and incubated for 24 hours. The cells were then incubated for a further 24 hours with or without paclitaxel or vinblastine (0.1 μM each), and cell viability was quantified through MTT incorporation, which is an indicator of mitochondrial activity, on an ELISA plate reader at 570 nm. The absorbance at 570 nm is proportional to the relative abundance of living cells. MTT assays were performed in triplicate in three experiments.

Tumorigenic Potential of Human Renal Tumor-Initiating Cells in Severe Combined Immunodeficient (SCID) Mice

$CD105^+$ CSCs and rhIL-15-EP were harvested by incubation with trypsin–EDTA, washed with PBS, counted in a microcytometer chamber, and resuspended in 100 μL of DMEM. Aliquots of 1×10^2 or 1×10^4 cells were added to 100 μL of Matrigel (BD Biosciences), chilled on ice, and injected subcutaneously with a 1-mL syringe fitted with a 26-gauge needle into the left and right sides of 6-week-old male SCID mice (Charles River, Jackson Laboratories, Bar Harbor, ME). Four mice were injected bilaterally with $CD105^+$ CSCs, and six mice were injected bilaterally with rhIL15-EP; we performed three independent experiments. At 3 ($CD105^+$ CSC group) or 6 (rhIL-15-EP group) weeks after cell injections, the mice were killed by carbon dioxide asphyxiation, and their tumors were excised, weighed, and measured. Studies were approved by the Italian Ministry of Health and by the Institutional Review Board of the University of Turin and were performed in accordance with the *National Institutes of Health Guide for the Care and Use of Laboratory Animals* (Institute of Laboratory Animal Resources: 7th ed. Washington, DC, Institute of Laboratory Animal Resources, Commission on Life Sciences, National Research Council, 1996).

Statistical Analysis

For the mouse tumor studies, the number of mice per group was based on our acquired expertise after 4 years of experiments with this model (we did not perform power calculations to determine the number of mice per group). The unit of analysis was the mouse, and the average of all tumors per mouse was taken into account. The Student *t* test was used to compare groups. All statistical tests were two-sided. A *P* value less than .05 was considered statistically significant.

Results

IL-15R Expression in Human Renal CSCs

We first investigated IL-15R expression on $CD105^+$ CSCs, using RPTECs as control. Flow cytometry revealed that $CD105^+$ CSCs and RPTECs express the three IL-15 receptor subunits—IL-15Rα, IL-15Rβ, and IL-15Rγ—on their cell surface (Figure 1, A). Immunoblot analysis of $CD105^+$ CSC lysates confirmed that these cells express the IL-15Rβ (75 kDa) and IL-15Rγ (60 kDa) chains as

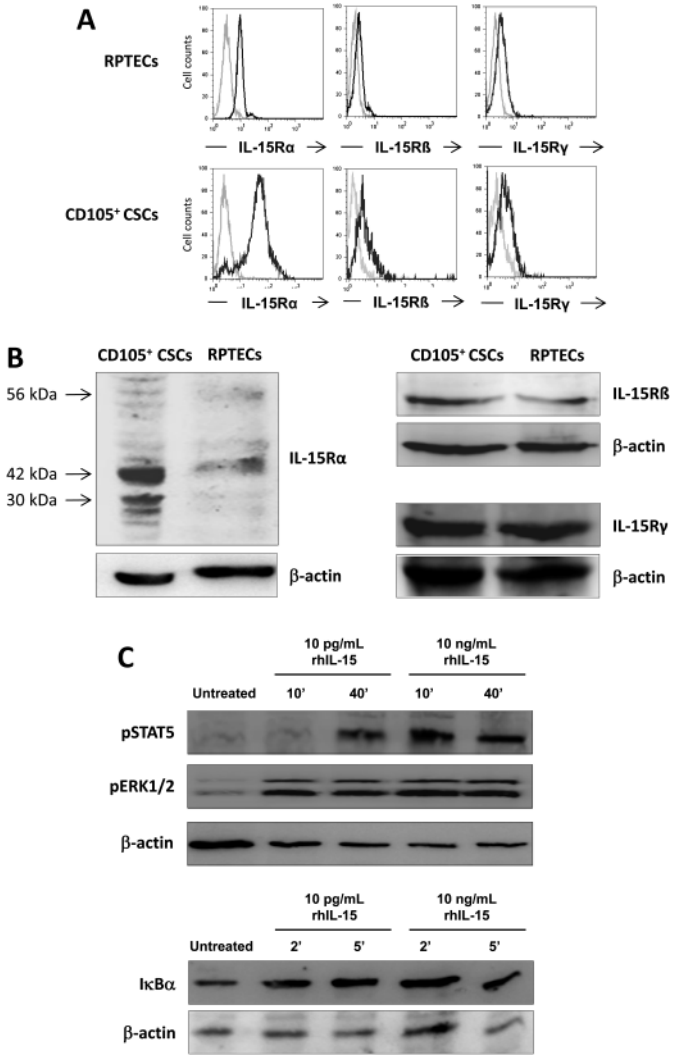

Figure 1. Analysis of IL-15R expression in human renal cancer stem cells (CSCs). CD105-positive human renal ($CD105^+$) CSCs and normal renal tubular epithelial cells (RPTECs; used as a control) (22) were subjected to fluorescence-activated cell sorting (FACS) and or immunoblot analysis to assess expression of IL-15Rα, IL-2Rβ, and IL-2Rγ. Results are representative of those obtained in three experiments. **A**) FACS analysis. **Black histograms** correspond to cells incubated with the IL-15 receptor–specific antibody, and **gray histograms** correspond to cells incubated with the isotype-matched control antibody. **B**) Immunoblot analysis. **C**) Expression of signal transduction proteins. Activation of MAPK ERK1/2 (pERK1/2) and STAT5 (pSTAT5) (upper panel) and IκBα (pIκBα) (lower panel) in $CD105^+$ CSCs stimulated with physiological (10 pg/mL) and supraphysiological (10 ng/mL) concentrations of recombinant human IL-15 (rhIL-15) was examined by immunoblotting using phosphorylation-specific antibodies. Each lane in (**B**) and (**C**) contains an equal amount of protein from whole-cell lysates. Immunoblotting for β-actin was used as a control for equal protein loading and transfer. IL-15 = interleukin 15.

well as various IL-15Rα isoforms ranging from 30 to 56 kDa in size (Figure 1, B).

We next evaluated the functionality of the IL-15R expressed on CD105$^+$ CSCs by using immunoblot analysis to examine expression of signal transduction proteins in cells incubated with physiological (10 pg/mL) and supraphysiological (10 ng/mL) concentrations of rhIL-15. Both concentrations of rhIL-15 induced the phosphorylation of MAP kinase ERK1/2 after 10–40 minutes, whereas STAT5 phosphorylation did not appear to be induced by the low IL-15 concentration at the 10-minute time point but was induced after 40 minutes of incubation. By contrast, treatment with 10 ng/mL of IL-15 induced STAT5 phosphorylation at both the 10- and 40-minute time points (Figure 1, C). Rapid IκBα phosphorylation, a key event in the activation of the transcription factor NF-κB, was also observed after 2–5 minutes of exposure to both concentrations of rhIL-15, confirming that this cytokine activated the classical IL-15 signal transduction pathways in CD105$^+$ CSCs.

Effect of rhIL-15 on Epithelial Differentiation of CD105$^+$ CSCs

CD105$^+$ CSCs maintain their stem cell properties in vitro when they are expanded in complete DMEM-LG (6). When CD105$^+$ CSCs are transferred to RPMI medium (with 10% FCS) lacking growth factors, they differentiate into epithelial cells within 3 weeks (6). Because IL-15 plays a major role in renal homeostasis by transmitting a survival signal (17,22) and preserving the expression of epithelial markers in RPTECs (J. Giron-Michel, S. Azzi, P. Eid, B. Azzarone, unpublished data), we investigated the effects of a physiological concentration of this cytokine (ie, 10 pg/mL) on the ability of CD105$^+$ CSCs to differentiate into epithelial cells. The cells were incubated for 4 weeks in complete DMEM-LG containing 10 pg/mL of rhIL-15, and a comparative time course analysis was performed by flow cytometry, to analyze expression of CD105, Nestin, Oct-3/4, and Nanog, stem cell markers required for the maintenance of pluripotency and the self-renewal of embryonic stem cells (23,24), and of two epithelial cell markers (E-cadherin and cytokeratins) (Figure 2, A). Expression of the four stem cell markers decreased during the first 2 weeks of incubation with rhIL-15. Expression CD105 and Nestin essentially disappeared during the third week of incubation with rhIL-15, whereas the loss of Nanog expression occurred during the fourth week of incubation, coinciding with a decrease in Oct-3/4 expression. In addition, rhIL-15 induced expression of E-cadherin and cytokeratins within 2 weeks of incubation. The expression of these markers continued to increase until the fourth week of incubation with rhIL-15. It is interesting that the expression of the four stem cell markers in rhIL-15-treated CSCs decreased strongly over the first week of treatment: Cells expressing these markers appeared as single homogenous peaks on flow cytometry histograms (Figure 2, A), suggesting the absence of IL-15-resistant CSC subsets. The loss of stem cell marker expression and the induction of epithelial marker expression during rhIL-15 treatment were confirmed by immunoblot analysis (Figure 2, B). These findings demonstrate that rhIL-15 induces, within 4 weeks, the epithelial differentiation of CD105$^+$ CSCs (to rhIL-15-EP). These newly differentiated cells express an epithelial phenotype similar to that observed when epithelial differentiation of CD105$^+$ CSCs is obtained in 3 weeks after switch to RPMI medium (Supplementary Figure 1, available online).

Endogenous IL-15 and CD105$^+$ CSC Epithelial Differentiation in RPMI Medium

Given that rhIL-15 induces the epithelial differentiation of CD105$^+$ CSCs maintained in complete DMEM-LG, we investigated if this cytokine was somehow involved in the epithelial differentiation obtained by switching CD105$^+$ CSCs to RPMI culture medium (Supplementary Figure 1, available online). For this purpose, we first investigated IL-15 secretion by CD105$^+$ CSCs all along the differentiation process in RPMI medium by subjecting cell supernatants harvested weekly to an ELISA assay. RCC and RPTECs were used as negative (25) and positive (15) controls, respectively. RPTECs secreted 15 pg/mL of IL-15 per 10^6 cells, whereas RCC and CD105$^+$ CSCs did not secrete detectable amounts of this cytokine (Figure 2, C). Notably, during the first week of culture in RPMI medium, CD105$^+$ CSCs acquired expression of the epithelial markers E-cadherin and pan-CK (Supplementary Figure 1, available online) and the ability to secrete small but detectable amounts of IL-15 (mean IL-15 secreted: 2 pg/mL per 10^6 cells, 95% confidence interval [CI] = 1.37 to 2.22 pg/mL). The amount of IL-15 secreted by the cells increased during the second and third week of culture (to a mean value of 5 pg/mL per 10^6 cells, 95% CI = 4.46 to 5.43 pg/mL), when these cells had undergone epithelial differentiation.

On the basis of these results, we investigated whether IL-15 production by CD105$^+$ CSCs cultured in RPMI medium was involved in the epithelial differentiation process. Neutralization of IL-15 by adding the anti-IL-15 blocking monoclonal antibody M111 to 1-week-old RPMI cell cultures completely inhibited CD105$^+$ CSC epithelial differentiation within 5 days, preserved the expression of stem cell markers (CD105, Nestin, Oct-3/4, Nanog), and prevented the expression of epithelial markers (E-cadherin and cytokeratins) (Figure 2, D). By contrast, CD105$^+$ CSCs treated with the monoclonal antibody did not show loss of stem cell markers nor acquisition of epithelial markers (Supplementary Figure 2, available online). Thus, the acquisition of IL-15 secretion is a key event in the epithelial differentiation of CD105$^+$ CSCs obtained by switching these cells to RPMI medium.

Effects of rhIL-15 Withdrawal on the Phenotype of rhIL-15-EP

We investigated the effect of withdrawing rhIL-15 on the differentiated epithelial phenotype by expanding 4-week-old rhIL-15-EP for an additional 2 weeks in complete DMEM-LG medium without addition of rhIL-15 (resulting in rhIL-15-EP6w). Two weeks of IL-15 starvation did not induce the re-expression of stem cell markers or the loss of epithelial markers as assessed by flow cytometry (Figure 3, A), suggesting that the rhIL-15-induced epithelial differentiation of CD105$^+$ CSCs was stable.

To evaluate whether rhIL-15-EP6w had the potential to form a polarized epithelium, a characteristic of fully differentiated epithelial cells, we analyzed cell phenotype, morphology, and cytoskeletal organization in immunofluorescence assays of specific markers. The rhIL-15-EP6w expressed neither the mesenchymal

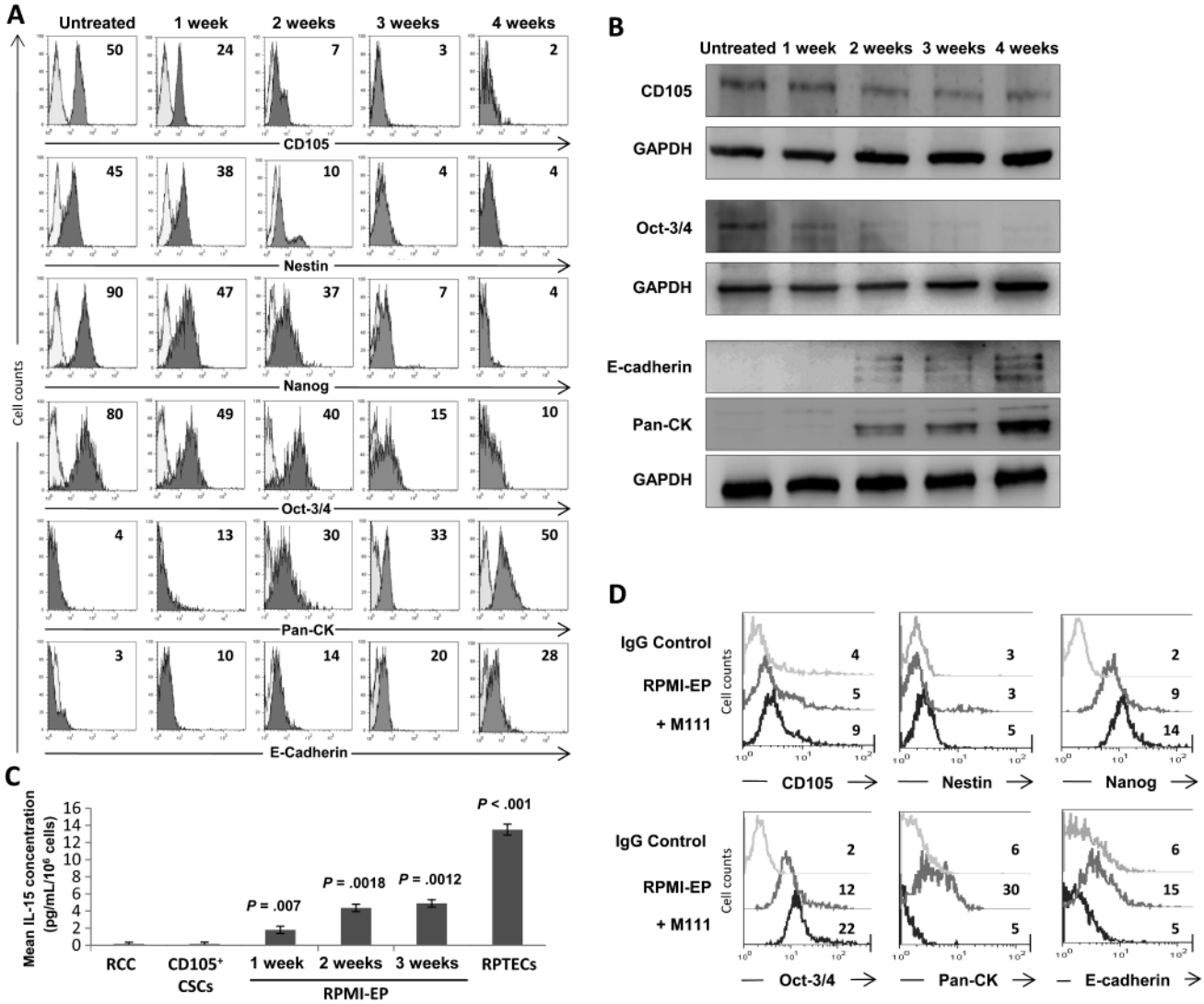

Figure 2. Epithelial differentiation of CD105-positive human renal cancer stem cells (CD105$^+$ CSCs) in the presence of recombinant human IL-15 (rhIL-15). CD105$^+$ CSCs treated with 10 pg/mL of rhIL-15 in complete low-glucose Dulbecco's modified Eagle medium were subjected to fluorescence-activated cell sorting (FACS) and immunoblot analysis to assess expression of stem cell (CD105, Nestin, Nanog, and Oct-3/4) and epithelial (E-cadherin, pan-cytokeratins) markers. Results in panels (**A**), (**B**), and (**D**) are representative of three experiments. **A**) FACS analysis of 10 000 events. **Black histograms** correspond to cells incubated with the antigen-specific antibody, and **gray histograms** correspond to cells incubated with the isotype-matched control antibody. Mean fluorescence intensity values for each marker are shown in the upper right of each histogram. **B**) Immunoblot analysis. Each lane contains an equal amount of protein from whole-cell lysates. Immunoblotting for glyceraldehyde 3-phosphate dehydrogenase (GAPDH) was used as a control for equal protein loading and transfer. **C**) Enzyme-linked immunosorbent assay of secreted IL-15 in RPMI-EP (CD105 ± CSCs differentiated in RPMI medium) cell supernatants. Primary cultures of human renal clear cell carcinomas (RCC), which do not secrete IL-15, were used as a negative control (25), and primary normal human renal epithelial cells (RPTECs) were used as a positive control (22). *P* values are two-sided (Student *t* test). **Data** represent mean values of three replicates in three independent experiments; **error bars** correspond to 95% confidence intervals. **D**) FACS analysis of 10 000 events to investigate the effect after 5 days of IL-15 neutralization on a 1-week-old RPMI cell culture using monoclonal antibody M111 (10 µg/mL). **Black** and **dark gray histograms** correspond to cells in the presence and absence, respectively, of M111, and **light gray histograms** correspond to cells incubated with the isotype-matched control antibody. Mean of fluorescence intensity values for each marker are shown on the right of each histogram. IgG = immunoglobulin G; IL-15 = interleukin 15.

markers CD105 and CD90 nor the stem cell markers Nanog and Nestin (Figure 3, B). Weak Oct-3/4 expression was detected only in the nucleolus of rhIL-15-EP6w. This subnuclear localization has been identified as a possible mechanism of Oct-3/4 inactivation (26). By contrast, immunofluorescence staining of the CD105$^+$ CSCs revealed expression of Nestin, a class VI intermediate filament protein found in stem cells (24), and CD105, mainly in the cytoplasm and at the cell surface (24). By contrast, staining for the transcription factors Oct-3/4 and Nanog was found preferentially in the nuclei. CD105$^+$ CSCs displayed no staining for the epithelial markers (E-cadherin and cytokeratins), whereas rhIL-15-EP6w displayed marked E-cadherin expression at cell borders, cytoplasmic cytokeratin staining, and abundant staining for zonula occludens-1 (a tight junction protein) (Figure 3, B). Rhodamine-conjugated phalloidin staining revealed a regular polygonal arrangement of rhIL-15-EP6w as shown by the dense peripheral distribution of F-actin (27). In addition, rhIL-15-EP6w expressed villin, an F-actin bundling protein of microvilli whose expression is

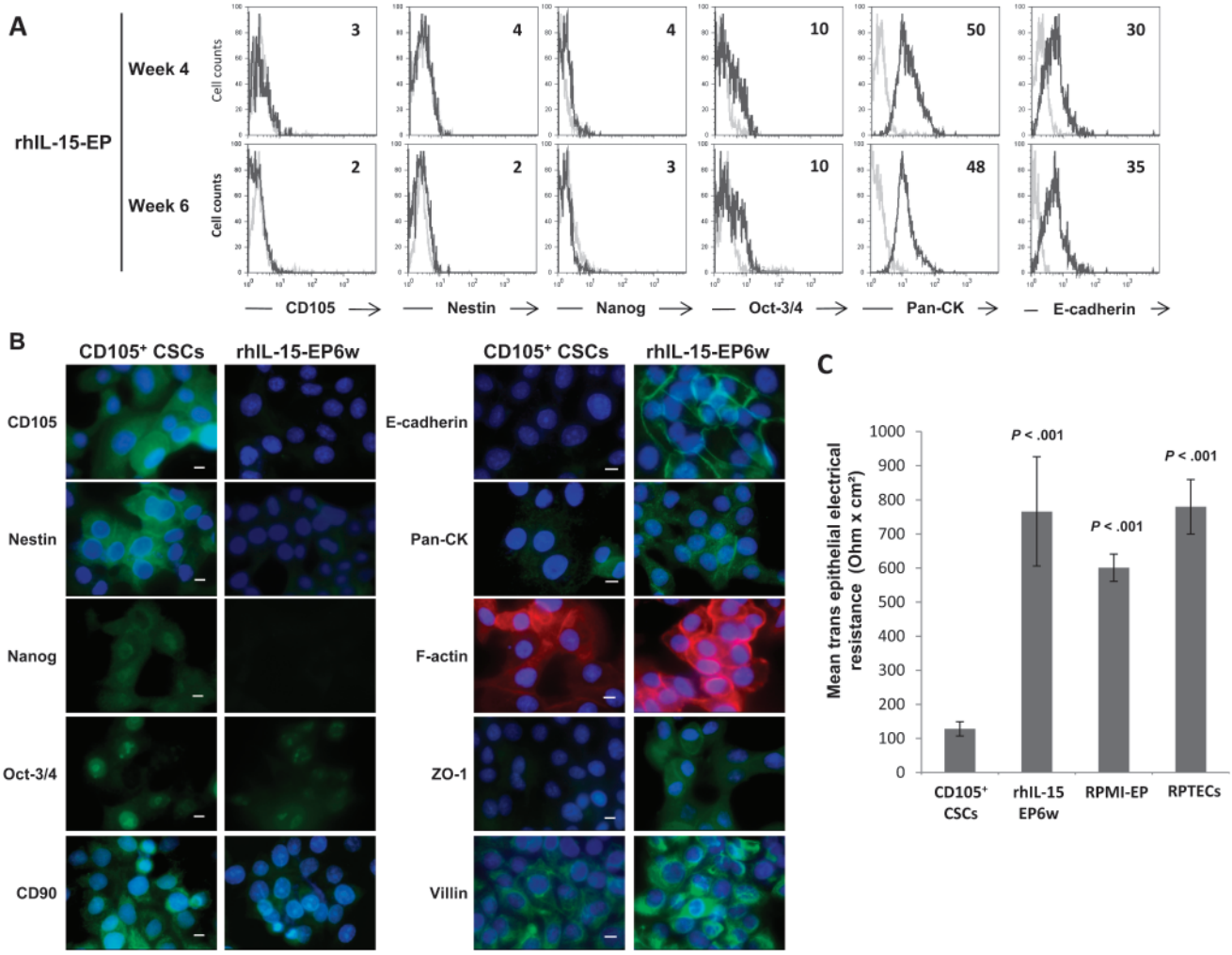

Figure 3. Analysis of functional polarity of differentiated CD105-positive human renal cancer stem cells (CD105$^+$ CSCs) induced by interleukin 15 (IL-15). CD105$^+$ CSCs treated for 4 weeks with recombinant human IL-15 (rhIL-15) (week 4) were expanded for an additional 2 weeks in the absence of the cytokine (week 6) and were subjected to fluorescence-activated cell sorting (FACS) and immunofluorescence staining to assess the expression of stem cell (CD105, Nestin, Oct-3/4, Nanog) and epithelial (E-cadherin, pan-CK) markers. Results in panels (**A**) and (**B**) are representative of three experiments. **A**) FACS analysis of 10000 events. **Black histograms** correspond to cells incubated with the antigen-specific antibody, and **gray histograms** correspond to cells incubated with the isotype-matched control antibody. The mean of fluorescence intensity value for each marker is shown in the upper right of each histogram. **B**) Immunofluorescence analysis. CD105$^+$ CSCs and CD105$^+$ CSCs treated for 4 weeks with rhIL-15 then expanded for an additional 2 weeks in the absence of the cytokine (rhIL-15-EP6w) were stained with antibodies to assess the expression of stem cell (CD105, Nestin, Oct-3/4, Nanog), mesenchymal (CD90), and epithelial (F-actin, E-cadherin, pan-CK, ZO-1, and villin) markers. Scale bar = 5 μm. **C**) Transepithelial electrical resistance assay. Confluent CD105$^+$ CSCs, undifferentiated or differentiated (rhIL-15-EP6w or RPMI-EP), were plated on Transwell filters, and their transepithelial electrical resistance was assessed with an epithelial volt-ohm meter. Tubular epithelial cells (RPTECs) were used as a positive control. Mean values, in ohms × cm^2, are plotted for three experiments; **error bars** correspond to 95% confidence intervals. *P* values are two-sided (Student *t* test).

restricted to polarized renal proximal tubular epithelial cells with a brush border (28), suggesting the polarization of rhIL-15-EP6w.

We next measured transepithelial electrical resistance—a technique that is widely used in functional analyses of the tight junction dynamics of epithelial barriers—to examine whether rhIL-15-EP6w had attained functional polarization (Figure 3, C). Transepithelial electrical resistance across confluent cellular monolayers of CD105$^+$ CSCs, rhIL-15-EP, RPMI-EP, or RPTECs was measured in a commercially available electrode chamber. Compared with undifferentiated CD105$^+$ CSCs, which exhibited a low transepithelial electrical resistance (128 ohm × cm^2), rhIL-15-EP6w and RPMI-EP exhibited statistically higher transepithelial electrical resistance (rhIL-15-EP6w: 766 ohm × cm^2, difference = 638 ohm × cm^2, 95% CI = 558.39 to 717.6 ohm × cm^2, $P < .001$; RPMI-EP: 601 ohm × cm^2, difference = 473 ohm × cm^2, 95% CI = 449.64 to 496.35 ohm × cm^2, $P < .001$), as did the positive control (RPTECs: 780 ohm × cm^2, difference = 652 ohm × cm^2, 95% CI = 621.21 to 682.78 ohm × cm^2, $P < .001$). These data suggest that both types of CSC-derived epithelial cells form a highly polarized functional monolayer.

Role of IL-15 in the Maintenance of the Epithelial Phenotype of Differentiated cells

IL-15 secretion is a hallmark of renal epithelial cells (13,14,17). We therefore investigated whether rhIL-15-EP, like RPMI-EP (Figure 2, C), could produce and secrete IL-15. We allowed 4-week-old rhIL-15-EP cultures to expand for a further 2 weeks in

complete DMEM-LG in the absence of rhIL-15. We then performed ELISA for IL-15 on the medium from those cells (rhIL-15-EP6w) to measure the secreted IL-15 (Figure 4, A). The amount of IL-15 secreted by rhIL-15-EP6w (14.5 pg/mL per 10^6 cells, 95% CI = 13.4 to 15.9) was similar to the amount secreted by an equal number of RPTECs (15 pg/mL per 10^6 cells, 95% CI = 14.9 to 18.1). Thus, all differentiated RPMI-EP and rhIL-15-EP were able to produce IL-15. Moreover, flow cytometry analysis showed that rhIL-15-EP6w as well as RPTECs expressed the IL-15R α, β, and γ chains (Figure 4, B), suggesting that they are able to activate endogenous IL-15-dependent autocrine–paracrine loops.

We investigated the involvement of secreted IL-15 in maintenance of the epithelial phenotype of rhIL-15-EP6w by adding the anti-IL-15-neutralizing monoclonal antibody M111 to the culture medium. Within 5 days after the addition of M111, we observed a loss of E-cadherin and cytokeratin expression and the reacquisition of expression of the stem cell markers Oct-3/4 and Nanog

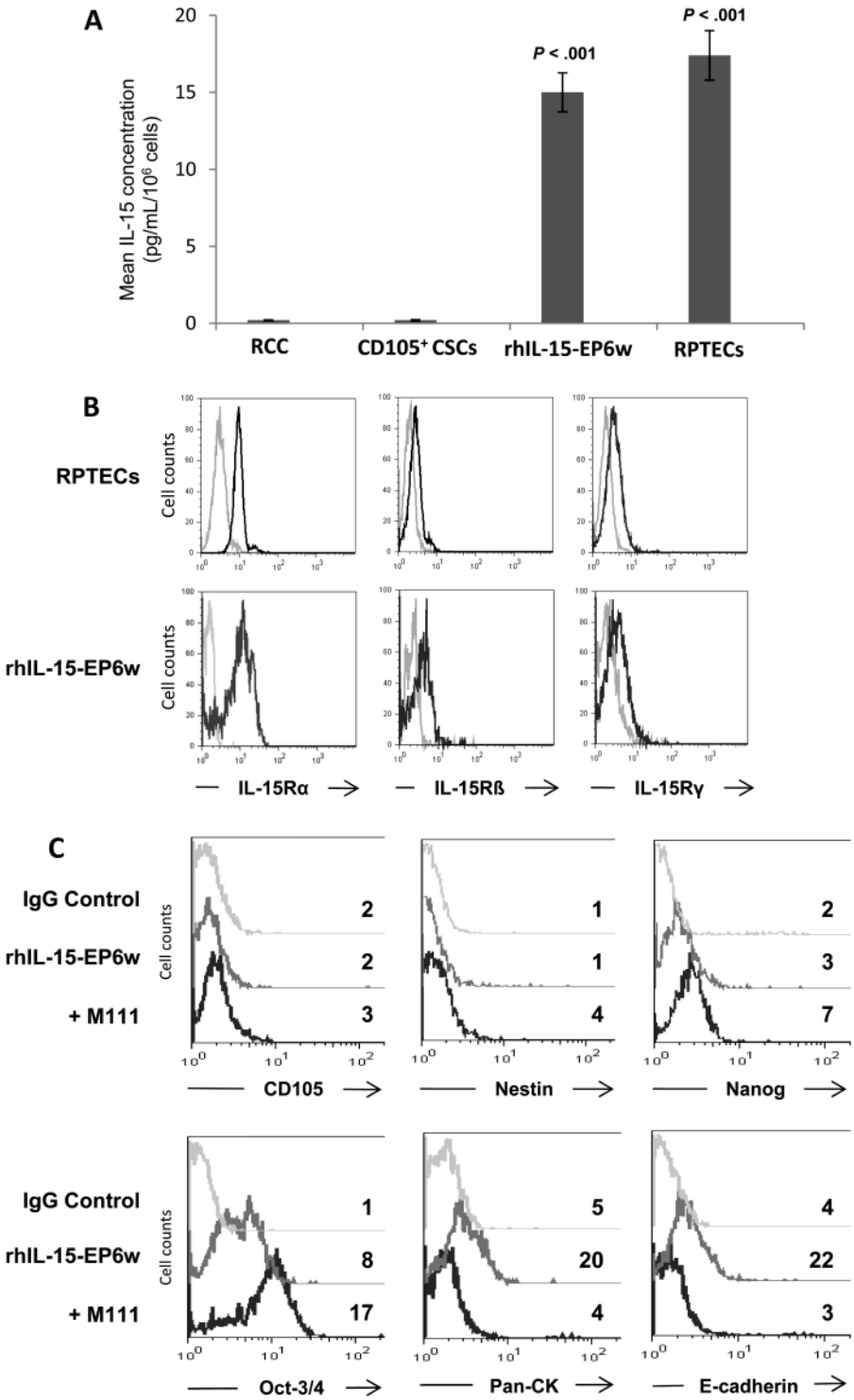

Figure 4. Involvement of interleukin 15 (IL-15) in the preservation of the epithelial phenotype. **A**) Enzyme-linked immunosorbent assay of secreted IL-15 in supernatants of CD105-positive human renal cancer stem cells ($CD105^+$ CSCs) and rhIL-15-EP6w. Primary cultures of human renal clear cell carcinomas (RCC), which do not secrete IL-15, were used as a negative control (25), and primary normal human renal epithelial cells (RPTECs) were used as a positive control (22). *P* values are two-sided (Student *t* test). **Data** represent mean values of three replicates in three independent experiments; **error bars** correspond to 95% confidence intervals. **B**) Fluorescence-activated cell sorting (FACS) analysis of expression of IL-15R α, β, and γ subunits by rhIL-15-EP6w. **Black histograms** correspond to cells incubated with the antigen-specific antibody, and **gray histograms** correspond to cells incubated with the isotype-matched control antibody. RPTECs were used as a positive control. Results are representative of three experiments. **C**) FACS analysis of 10 000 events to investigate the effect after 5 days of IL-15 neutralization on rhIL-15-EP6w cultures using IL-15-neutralizing monoclonal antibody M111 (10 μg/mL). **Black** and **dark gray** histograms correspond to cells incubated in the presence and absence, respectively, of M111, and **light gray histograms** correspond to cells incubated with the isotype-matched control antibody. The mean of fluorescence intensity values for each marker are shown on the right of each histogram.

(Figure 4, C). These findings indicate that IL-15 autocrine–paracrine loops play a role in the epithelial homeostasis of differentiated cells, even after the withdrawal of long-term rhIL-15 treatment (Figure 3, A). $CD105^+$ CSCs, which do not secrete IL-15, were used as control of the specificity of action of the M111 antibody; the antibody had not effect on the phenotype of these cells (Supplementary Figure 2, available online).

Sensitivity of $CD105^+$ CSCs, RPMI-EP, and rhIL-15-EP to Cytotoxic Drugs

CSCs are more resistant to conventional chemotherapy compared with differentiated cancer cells (5). We therefore examined the effect of rhIL-15-mediated differentiation on sensitivity of $CD105^+$ CSCs to vinblastine or paclitaxel (0.1 μM each), two of the principal cytotoxic drugs used in chemotherapy for renal carcinoma. $CD105^+$ CSCs undergoing epithelial differentiation by treatment with rhIL-15 (0–4 weeks) as well as RPMI-EP were treated with vinblastine or paclitaxel for 24 hours and then subjected to the MTT assay to measure cell viability. $CD105^+$ CSCs were almost totally resistant to vinblastine or paclitaxel (80% cell viability after exposure to either drug) (Figure 5, A), whereas cells treated for 4 weeks with rhIL-15 displayed increased sensitivity to vinblastine (cell viability = 40%, difference = 40%, 95% CI = 38.58% to 41.41%, $P < .001$) and to paclitaxel (cell viability = 43%, difference = 37%, 95% CI = 35.58% to 38.41%, $P < .001$). Compared with $CD105^+$ CSCs, RPMI-EP also displayed increased sensitivity to vinblastine and paclitaxel (cell viability $CD105^+$ CSCs vs RPMI-EP, vinblastine: 80% vs 45%, difference = 35%, 95% CI = 32.17% to 37.82%, $P < .001$; paclitaxel: 80% vs 47%, difference = 33%, 95% CI = 30.17% to 35.82%, $P < .001$).

We next carried out cell cycle analysis to determine whether the observed decrease in viability with drug treatment was associated with the induction of cell death (Figure 5, B). Flow cytometry analysis showed that, in the absence of the chemotherapy drugs, $CD105^+$ CSCs treated with rhIL-15 (0–4 weeks) or not treated displayed no detectable apoptotic cells (as assessed by determining the numbers of hypodiploid cells in the sub-G_1 phase of the cell cycle). Both drugs (at 0.1 μM each) induced low levels of apoptosis in $CD105^+$ CSCs (mean percentage of apoptotic cells, vinblastine: 16.5%; paclitaxel: 11.6%). By contrast, both drugs induced statistically significant higher levels of apoptosis during rhIL-15-induced epithelial differentiation of $CD105^+$ CSCs (eg, at the fourth week of rhIL-15 treatment, mean percentage of apoptotic cells, vinblastine: 33%, difference = 16.5%, 95% CI = 12.25% to 20.74%, $P = .0025$; paclitaxel: 35%, difference = 23.4%, 95% CI = 22.5% to 24.24%, $P = .0015$). Treatment of differentiated RPMI-EP with vinblastine or paclitaxel also induced statistically significant higher levels of apoptosis compared with vinblastine- or paclitaxel-treated $CD105^+$ CSCs (mean percentage of apoptotic cells, vinblastine: 32%, difference = 15.5%, 95% CI = 11.25 to 19.74, $P = .0092$; paclitaxel: 30.4%, difference = 18.8%, 95% CI = 18.23 to 19.36, $P = .0026$). Thus, the acquisition of a higher sensitivity to these cytotoxic agents was associated with the epithelial differentiation process.

CSCs employ several mechanisms to protect them against cytotoxic agents. One of these mechanisms involves the production of large amounts of ABC transporters, which are responsible for the efflux of xenobiotics across cell membranes against a concentration gradient. We used the Hoechst dye exclusion assay (20) to assess the efflux activity of $CD105^+$ CSCs, RPMI-EP, and rhIL-15-EP. Cells were stained with the fluorescent dye Hoechst 33342 in the presence and absence of the calcium channel blocker, verapamil, which inhibits efflux activity. The cells were washed to remove unincorporated dye and subjected to flow cytometry with sorting for DNA content. An overlay of the histograms for $CD105^+$ CSCs in the presence and absence of verapamil revealed the existence of a subset of cells in the G_0/G_1 population with high dye efflux activity (red circle in Figure 5, C) that disappeared after treatment with verapamil, an ABC transporter inhibitor. By contrast, overlays of the histograms for RPMI-EP and rhIL-15-EP in the presence and absence of verapamil did not reveal the existence of subsets of highly effluxing cells, indicating an absence of ABC transporters activity in both types of differentiated cells, consistent with the loss of this cytoprotective mechanism during differentiation.

High levels of the detoxifying enzyme ALDH can also provide tumors with a mechanism for resisting the effects of chemotherapy (29). We therefore investigated whether the expression of ALDH, a stem cell marker for both normal and malignant stem and progenitor cells (29), decreased during differentiation (Figure 5, D). ALDH activity in $CD105^+$ CSCs, rhIL-15EP, and RPMI-EP was measured by flow cytometry with the use of an ALDEFLUOR kit. $CD105^+$ CSCs displayed ALDH activity, whereas no ALDH activity was detected in RPMI-EP and rhIL-15-EP. The loss of ABC transporters and ALDH activity may account, in part, for the greater susceptibility of differentiated cells to cytotoxic agents.

Tumorigenic Properties of $CD105^+$ CSCs, RPMI-EP, and rhIL-15–EP

We next investigated whether the epithelial differentiation of $CD105^+$ CSCs was associated with a loss of the tumorigenic properties that are typical of CSCs (ie, the ability to form spheroids in culture and induce tumor development in immunosuppressed mice). We first assessed the ability of these cells to grow as floating spheroids. $CD105^+$ CSCs and cells treated for 2 weeks with rhIL-15 formed large spheroids when grown in nonadherent culture conditions, whereas rhIL15-EP had lost this property after 4 weeks of differentiation (data not shown).

We then investigated whether the epithelial differentiation of $CD105^+$ CSCs was associated with a loss of tumorigenicity. We found that bilateral subcutaneous injection of 10^2 $CD105^+$ CSCs into SCID mice induced the formation of large (2 × 2 cm) tumors within 3 weeks after injection in all mice studied (n = 4 mice; experiments repeated three times), whereas the bilateral injection of either 10^2 or 10^4 rhIL-15-EP (n = 6 mice per group; experiments repeated three times) did not result in any tumor development, even by 6 weeks after injection. Thus, rhIL-15-EP has no in vivo tumorigenic potential.

Effect of rhIL-15 on Self-Renewal of $CD105^+$ CSCs

Self-renewal is a mechanism required for preservation of the CSCs pool that involves the generation, by asymmetric division, of one daughter cell that replaces the original CSCs and second daughter cell that is destined to differentiate (30). It was therefore important to evaluate the possible effects of rhIL-15 on both of these daughter

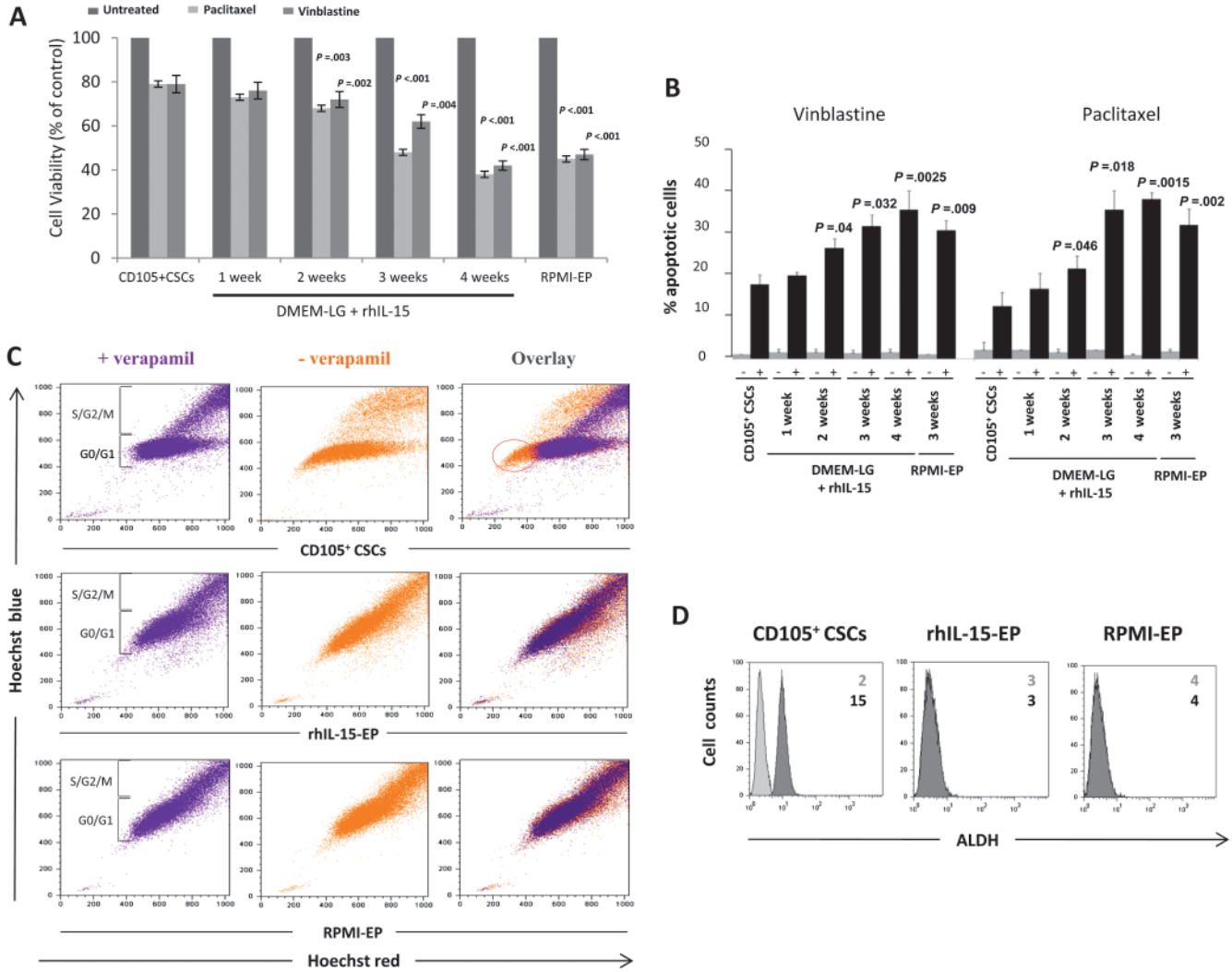

Figure 5. Sensitivity of RPMI-EP and rhIL-15-EP to cytotoxic drugs. **A**) Cell viability assay. The sensitivity of RPMI-EP and CD105-positive human renal cancer stem cells (CD105$^+$ CSCs) during recombinant human IL-15 (rhIL-15)–induced epithelial differentiation (0–4 weeks) in complete low-glucose Dulbecco's modified Eagle medium to cytotoxic drugs was evaluated by the MTT cell viability assay. Cells were treated for 24 hours with vinblastine or paclitaxel (0.1 μM each). Cell viability after drug treatment is presented as a percentage relative to untreated (control) cells. The mean values for three experiments are shown; **error bars** correspond to 95% confidence intervals. **B**) Cell cycle analysis of the effect of paclitaxel and vinblastine (0.1 μM each) on apoptosis in differentiated epithelial cells. The apoptotic cell fraction was plotted for cells treated with (**black bars**) and without (**gray bars**) paclitaxel or vinblastine. Mean values for three experiments are shown; **error bars** correspond to 95% confidence intervals. *P* values are two-sided (Student *t* test). **C**) Hoechst dye exclusion assay of ATP-binding cassette (ABC) transporter–dependent efflux activity. CD105$^+$ CSCs and differentiated RPMI-EP or rhIL-15-EP were stained with Hoechst 33342 dye and ABC transporter–dependent efflux activity (ie, as determined by dye retention) was evaluated by flow cytometry in cells that were (**purple**) or were not (**orange**) treated for 1 hour with verapamil (50 μM), a calcium channel blocker that inhibits efflux activity. The overlay reveals differences in the cell populations when efflux activity is inhibited. The standard flow cytometry–based assays involves analysis of the **blue** and **red light** emission of double-stranded DNA labeled with the Hoechst 33342 marker, making it possible to distinguish between the G_0/G_1 and $S/G_2/M$ cell populations and to determine the efflux activities of these two populations using the calcium channel blocker verapamil. The results are representative of three experiments. **D**) The aldehyde dehydrogenase (ALDH) activity in CD105$^+$ CSCs, rhIL-15-EP, or RPMI-EP was measured by flow cytometry (50 000 events), with the ALDEFLUOR kit. ALDH1 activity was measured in the absence (**black**) or presence (**gray**) of the specific ALDH inhibitor DEAB. One experiment representative of three is shown.

cell populations. We performed the Hoechst dye exclusion assay on CD105$^+$ CSCs (Figure 6, A, left and center panels), and identified, in the total G_0/G_1 population, a side population subset that has been reported to contain the most primitive CSCs pool (30,31). Flow cytometry with gating on the side population, the total G_0/G_1 population, and non–side population revealed that all three subsets responded to rhIL-15 stimulation by activating STAT5 phosphorylation (Figure 6, A, right panels). We also investigated the possible effects of IL-15 on CSC self-renewal by conducting limiting dilution assays of spheroid colony formation by CD105$^+$ CSCs in the presence and absence of rhIL-15 (Figure 6, B). After 3 weeks of culture, 43% of CD105$^+$ CSCs cultured in the absence of rhIL-15 produced spheroids compared with only 11% of rhIL-15-treated CD105$^+$ CSCs (difference 32%, 95% CI = 30.53% to 33.47%, $P = .012$). Thus, IL-15 blocks CSC self-renewal.

Hypoxia is a characteristic of the CSC microenvironment (niche) that is involved in the maintenance of stem cell fate, self-renewal, and multipotency of CSCs. We therefore investigated whether 24 hours of exposure to hypoxic conditions (1% O_2) had any effect on the response of CSCs to rhIL-15. We therefore

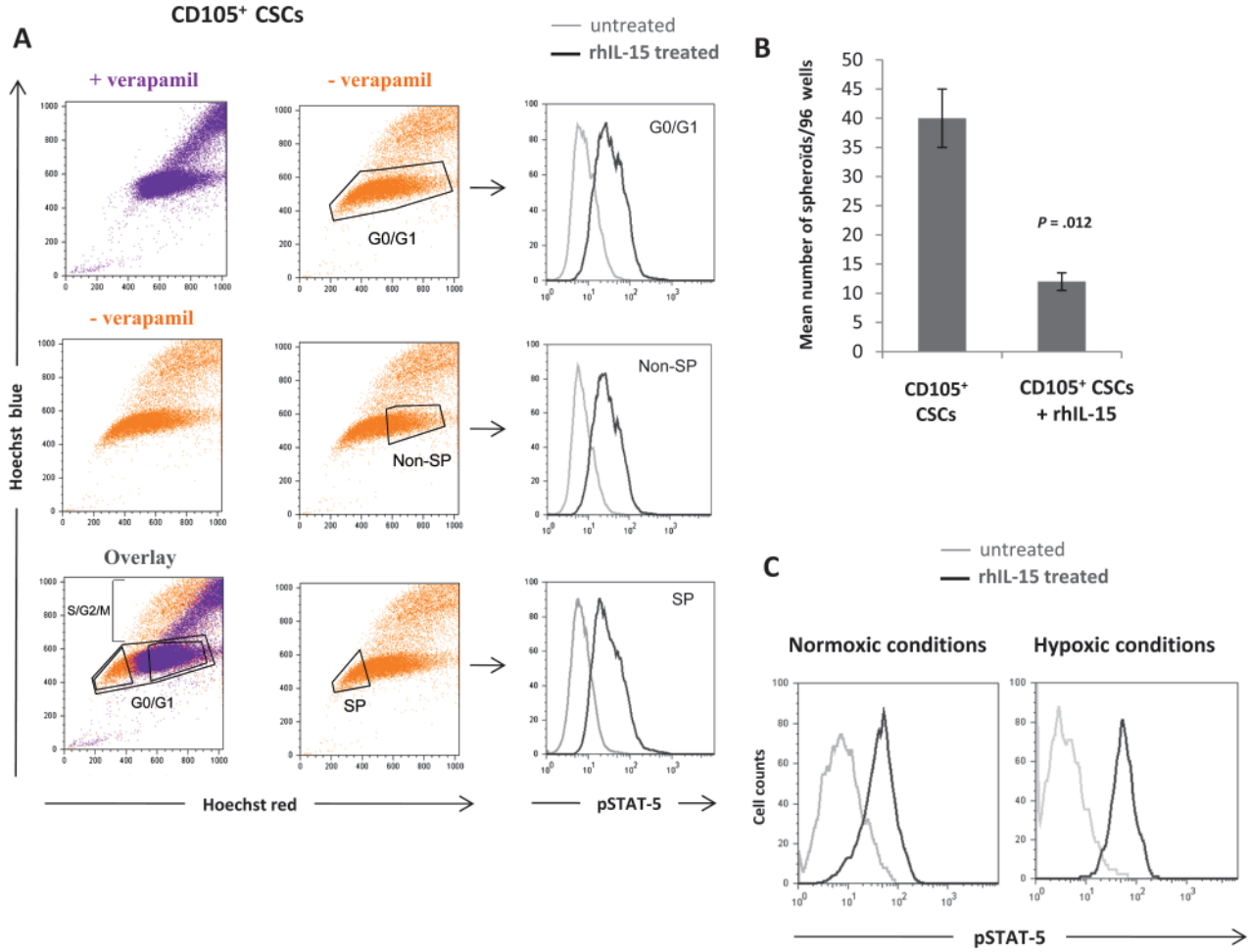

Figure 6. Role of recombinant human IL-15 (rhIL-15) in CD105-positive human renal cancer stem cell (CD105⁺ CSC) self-renewal. **A**) Interleukin 15 (IL-15)–dependent STAT5 activation in side population (SP) and non–side population cells. The SP was identified by staining with Hoechst 33342, making it possible to detect a distinct subpopulation of cells, derived from G_0/G_1 cells and having a large capacity for dye efflux. The SP can be distinguished from the non-SP subset, which consists principally of committed CSCs. To evaluate STAT5 activation in the SP and non-SP subsets, CD105⁺ CSCs were treated with 10 pg/mL of rhIL-15 during the last 45 minutes of Hoechst 33342 dye staining in the absence of verapamil. STAT5 phosphorylation was further analyzed by fluorescence-activated cell sorting analysis (50 000 events) in the three gates corresponding to the G_0/G_1, non-SP, and SP subsets. One experiment representative of three is shown. **B**) Sphere formation assay. We evaluated the effect of IL-15 on CD105⁺ renewal by carrying out a limiting dilution assay for spheroid formation. CSCs were plated at a density of one cell per well, in ultralow attachment 96-well plates containing complete low-glucose Dulbecco's modified Eagle medium (DMEM-LG) in the presence or absence of rhIL-15 (10 pg/mL). After 3 weeks, each well was examined under a light microscope, and the total number of wells with spheroid colonies was determined. **Data** represent mean values of three replicates for three experiments; **error bars** correspond to 95% confidence intervals. *P* values are two-sided (Student *t* test). **C**) Flow cytometry analysis of STAT5 activation in normoxic and hypoxic conditions. CD105⁺ CSCs were incubated for 24 hours in a hypoxia chamber in a humidified atmosphere containing 5% CO_2, 1% O_2, and 94% N_2, at 37°C and incubated for 45 minutes in the presence or absence of rhIL-15 (10 pg/mL) in complete DMEM-LG medium and analyzed by flow cytometry. **Light gray** histograms correspond to untreated cells, and **black histograms** correspond to rhIL-15-treated cells. One experiment representative of three is shown, with 50 000 events analyzed.

compared STAT5 activation induced by 10 pg/mL of rhIL-15 in CD105⁺ CSCs cultured in normoxic vs hypoxic conditions (Figure 6, C). Flow cytometry analysis showed that phosphorylation of STAT5 induced by rhIL-15 was not affected by hypoxic conditions, suggesting that hypoxia does not hinder the efficiency of rhIL-15 in CSC niches.

Discussion

We show here that IL-15, a cytokine that plays a major role in renal homeostasis (15,18,22), induces the stable epithelial differentiation of renal CD105⁺ CSCs generating a differentiated nontumorigenic cell population that is more sensitive to cytotoxic drugs compared with the parental CSCs. Renal cell carcinoma is a common urological tumor that is characterized by a high metastatic index at diagnosis, a high rate of relapse, and insensitivity to radiation and chemotherapy (12). CD105⁺ CSCs recently isolated from human renal cancer specimens are highly tumorigenic in vivo, such that as few as 10^2 CD105⁺ CSCs are sufficient to induce the development of serially transplantable tumors in SCID mice (6). Because CD105⁺ CSCs are highly resistant to cytotoxic drugs, alternative strategies are required to target these cells to ensure their effective eradication. This aim can be obtained through treatments based on either the elimination or differentiation of CSCs, which could render cells more sensitive to chemotherapy (32). Differentiation has been achieved with human CSCs derived from melanomas and

from mammary, prostatic, and renal carcinomas, by shifting the cells from their original medium to specific differentiation media (5,6,33–35).

In this study, we obtained epithelial differentiation of CD105$^+$ CSCs without shifting the cells to a specific differentiation medium but rather by maintaining the cells in complete DMEM-LG (which preserves in vitro their stem-like properties) in presence of rhIL-15. Furthermore, the epithelial differentiation achieved by shifting CD105$^+$ CSCs to RPMI medium was associated with the acquisition of IL-15 secretion. It is interesting that antibody-mediated neutralization of IL-15 secreted by CD105$^+$ CSCs inhibited their differentiation in RPMI medium, providing further evidence that IL-15 is a key inducer of epithelial differentiation. In vitro, IL-15 induced differentiation of CD105$^+$ CSCs into epithelial cells that had the morphological features, markers, and functions of polarized epithelial cells. Indeed, our data show that RPMI-EP and rhIL-15-EP each form a monolayer that is characterized by a cytoarchitecture (F-actin organization) that is typical of polarized epithelial cells and the expression of villin, a marker restricted to epithelia with a brush border. In addition, these differentiated cells express E-cadherin and ZO-1, two junction-associated proteins that confer high intercellular junction integrity (21). The integrity of the RPMI-EP and rhIL-15-EP monolayers was confirmed by their high levels of transepithelial electrical resistance. Furthermore, unlike CD105$^+$ CSCs, differentiated RPMI-EP and rhIL-15-EP secreted IL-15, a hallmark of epithelial cells (17,22). Neutralization of the secreted IL-15 using blocking antibodies caused the loss of epithelial markers and reacquisition of stem cell markers. These data demonstrate that endogenous IL-15, acting through autocrine–paracrine loops, plays a role in maintaining the epithelial phenotype of RPMI-EP and rhIL-15-EP.

Remarkably, we found that RPMI-EP and rhIL-15-EP were more sensitive than CD105$^+$ CSCs to renal carcinoma chemotherapy agents (vinblastine and paclitaxel). This finding suggests that epithelial differentiation may sensitize CSCs to cytotoxic stimuli. In differentiated cells, this sensitization to chemotherapy drugs was associated with decreases in ABC transporter expression and ALDH activity. In addition, the IL-15-induced differentiation of CD105$^+$ CSCs was associated with a loss of tumorigenic properties that are considered the hallmarks of CSCs, such as the ability to grow as nonadherent spheroids and to develop tumors in SCID mice.

Given our finding that IL-15 induces differentiation of CSCs in vitro, it remains unclear why CSCs persist in vivo, where expression of endogenous IL-15 is ubiquitous. Considering the important role of the normal stem cell niche in controlling cell fate determination, it has been suggested that CSCs likewise reside in a "CSC niche" where they are subject to mechanisms favoring self-renewal and the inhibition of differentiation (36). In this respect, limiting the intrarenal availability of IL-15 may be an important mechanism for maintaining CD105$^+$ CSCs in the tumor microenvironment and preventing their epithelial differentiation. This hypothesis is based on the fact that intrarenal IL-15 plays an important function in kidney homeostasis, as has been shown in IL-15$^{-/-}$ mice (15) and in renal diseases that involve the development of a hypoxic and/or inflammatory environment (37). In these models, a sharp decrease in intrarenal IL-15 rapidly results in epithelial injury and a loss of renal function that is not restored by increasing the levels of circulating IL-15 (15,37). In patients with renal cell carcinoma, a decreased intrarenal IL-15 availability is created by the constant hypoxia (38) and lack of IL-15 secretion by both the tumor cells (25) and CD105$^+$ CSCs, which creates a microenvironment of IL-15 starvation that prevents CSCs from differentiating.

Because the self-renewal of the CSC pool involves the generation, by asymmetric division, of a daughter cell to replace the original CSCs and a daughter cell that is destined for differentiation, it was important to evaluate the possible effects of rhIL-15 on cells committed to differentiation and on the most primitive subset of CSCs. The literature suggests that self-renewal is associated with Hoechst 33342–effluxing cells, which correspond to the most primitive CSCs, also named the side population (39). Hoechst dye exclusion assays showed that CD105$^+$ CSCs, even after 2 months in culture, included a side population and were able to form spheroids in clonogenic nonadherent culture conditions and to generate large tumors in SCID mice.

We found that the side population detected in CD105$^+$ CSCs underwent STAT5 phosphorylation in response to rhIL-15 stimulation, a response that was as efficient as that of the main CD105$^+$ CSC population. Moreover, this response occurred under normoxic as well as hypoxic conditions. Hypoxia is a constant characteristic of the CSCs niches involved in the maintenance of stem cell fate, self-renewal, and multipotency (38). In addition, we also found that rhIL-15-treated CSCs lost the capacity to generate spheroids in limiting dilution assays, suggesting that rhIL-15 blocked CSCs self-renewal. Thus, rhIL-15 acts on all CSCs subpopulations studied, including the CD105$^+$ side population subset. This conclusion is also supported by our observation that mice injected with rhIL-15-differentiated cells failed to develop tumors, even at doses as high as 10 000 cells per mouse and even by 6 weeks after injection, whereas mice injected with 100 undifferentiated CSCs developed large tumors by 3 weeks after injection.

These observations support the use of IL-15 in the treatment of renal carcinoma. A phase I study of intravenous rhIL-15 for the treatment of metastatic renal cancers has been initiated (clinicaltrials.gov trial identifier NCT01021059) based on the concept that IL-15 is an inducer of both innate and specific immunity (40). Indeed, IL-15 gene transfer (41,42) or systemic administration of recombinant IL-15 mediates the inhibition of tumor growth in mice (43) through the induction of CD8-positive T and/or NK cell responses. Importantly, systemic administration of recombinant IL-15 had fewer toxic effects compared with systemic administration of IL-2, which is commonly used in renal cancer treatment and produced no vascular leak syndrome in mice (42) or primates (44). In addition to this immunity-stimulating activity, we have shown that IL-15 has a direct effect on tumor cells, decreasing the size of the CD105$^+$ CSC pool and generating nontumorigenic epithelial cells that are more sensitive to chemotherapy. We propose two IL-15-based strategies to target CSCs. The first involves in vivo induction of paracrine IL-15 secretion by renal CSCs or neighboring cells mediated by plasmid gene transfer (41,42) and targeted delivery systems (45). The second strategy involves direct administration of IL-15 to the tumor tissue by means of autologous

dendritic cells, a major source of IL-15 (46), pulsed with tumor peptides (47,48), or direct delivery to the CSCs by coupling the cytokine to antibodies that target CSCs markers (eg, CD105). Given the potential dual effect of IL-15 on both the differentiation of renal CSCs and the activation of an antitumor immune response, this cytokine could provide the foundations of an interesting strategy for improving the treatment of renal carcinoma.

We acknowledge a limitation of this study. Although we have shown that, in vitro, IL-15 differentiates all $CD105^+$ CSCs without selection of IL-15-unresponsive subsets, we cannot exclude the possibility that, in vivo, some unknown microenvironmental parameters other than hypoxia (eg, cytokines, stromal cells) may limit IL-15 action inside the CSC niches.

In conclusion, our results show that IL-15 is a key factor that directs the epithelial differentiation of renal CSCs and also meets the criteria for major treatment strategies: Depletion of the CSC pool and generation of differentiated nontumorigenic cells with increased sensitivity to chemotherapeutic agents.

References

1. Singh SK, Clarke ID, Terasaki M, et al. Identification of a cancer stem cell in human brain tumors. *Cancer Res.* 2003;63(18):5821–5828.
2. Al-Hajj M, Wicha MS, Benito-Hernandez A, et al. Prospective identification of tumorigenic breast cancer cells. *Proc Natl Acad Sci U S A.* 2003; 100(7):3983–3988.
3. Bonnet D, Dick JE. Human acute myeloid leukemia is organized as a hierarchy that originates from a primitive hematopoietic cell. *Nat Med.* 1997;3(7):730–737.
4. Ricci-Vitiani L, Lombardi DG, Pilozzi E, et al. Identification and expansion of human colon-cancer-initiating cells. *Nature.* 2007;445(7123):111–115.
5. Hermann PC, Bhaskar S, Cioffi M, et al. Cancer stem cells in solid tumors. *Semin Cancer Biol.* 2010;20(2):77–84.
6. Bussolati B, Bruno S, Grange C, et al. Identification of a tumor-initiating stem cell population in human renal carcinomas. *FASEB J.* 2008;22(10): 3696–3705.
7. Ponti D, Costa A, Zaffaroni N, et al. Isolation and in vitro propagation of tumorigenic breast cancer cells with stem/progenitor cell properties. *Cancer Res.* 2005;65(13):5506–5511.
8. Keysar SB, Jimeno A. More than markers: biological significance of cancer stem cell-defining molecules. *Mol Cancer Ther.* 2010;9(9):2450–2457.
9. Zhou BB, Zhang H, Damelin M, et al. Tumour-initiating cells: challenges and opportunities for anticancer drug discovery. *Nat Rev Drug Discov.* 2009;8(10):806–823.
10. Tang C, Ang BT, Pervaiz S. Cancer stem cell: target for anti-cancer therapy. *FASEB J.* 2007;21(14):3777–3785.
11. Massard C, Deutsch E, Soria JC. Tumour stem cell-targeted treatment: elimination or differentiation. *Ann Oncol.* 2006;17(11):1620–1624.
12. Lane BR, Kattan MW. Predicting outcomes in renal cell carcinoma. *Curr Opin Urol.* 2005;15(5):289–297.
13. Budagian V, Bulanova E, Paus R, et al. IL-15/IL-15 receptor biology: a guided tour through an expanding universe. *Cytokine Growth Factor Rev.* 2006;17(4):259–280.
14. Huang YS, Cheng SN, Chueh SH, et al. Effects of interleukin-15 on neuronal differentiation of neural stem cells. *Brain Res.* 2009;1304(1): 38–48.
15. Shinozaki M, Hirahashi J, Lebedeva T, et al. IL-15, a survival factor for kidney epithelial cells, counteracts apoptosis and inflammation during nephritis. *J Clin Invest.* 2002;109(7):951–960.
16. Lamana A, Ortiz AM, Alvaro-Gracia JM, et al. Characterization of serum interleukin-15 in healthy volunteers and patients with early arthritis to assess its potential use as a biomarker. *Eur Cytokine Netw.* 2010;21(3):186–194.
17. Lewis E, Weiler M, Chaimovitz C, et al. Interleukin-15 is the main mediator of lymphocyte proliferation in cultures mixed with human kidney tubular epithelial cells. *Transplantation.* 2001;72(5):886–890.
18. Khawam K, Giron-Michel J, Gu Y, et al. Human renal cancer cells express a novel membrane-bound interleukin-15 that induces, in response to the soluble interleukin-15 receptor alpha chain, epithelial-to-mesenchymal transition. *Cancer Res.* 2009;69(4):1561–1569.
19. Giron-Michel J, Menard F, Negrini S, et al. EBV-associated mononucleosis does not induce long-term global deficit in T-cell responsiveness to IL-15. *Blood.* 2009;113(19):4541–4547.
20. Kobayashi I, Moritomo T, Ototake M, et al. Isolation of side population cells from ginbuna carp (Carassius auratus langsdorfii) kidney hematopoietic tissues. *Dev Comp Immunol.* 2007;31(7):696–707.
21. Sonoda S, Spee C, Barron E, et al. A protocol for the culture and differentiation of highly polarized human retinal pigment epithelial cells. *Nat Protoc.* 2009;4(5):662–673.
22. Tejman-Yarden N, Zlotnik M, Lewis E, et al. Renal cells express a functional interleukin-15 receptor. *Nephrol Dial Transplant.* 2005;20(3):516–523.
23. Loh YH, Wu Q, Chew JL, et al. The Oct4 and Nanog transcription network regulates pluripotency in mouse embryonic stem cells. *Nat Genet.* 2006;38(4):431–440.
24. Yang XH, Wu QL, Yu XB, et al. Nestin expression in different tumours and its relevance to malignant grade. *J Clin Pathol.* 2008;61(4):467–473.
25. Trinder P, Seitzer U, Gerdes J, et al. Constitutive and IFN-gamma regulated expression of IL-7 and IL-15 in human renal cell cancer. *Int J Oncol.* 1999;14(1):23–31.
26. Chin JH, Shiwaku H, Goda O, et al. Neural stem cells express Oct-3/4. *Biochem Biophys Res Commun.* 2009;388(2):247–251.
27. Musch MW, Walsh-Reitz MM, Chang EB. Roles of ZO-1, occludin, and actin in oxidant-induced barrier disruption. *Am J Physiol Gastrointest Liver Physiol.* 2006;290(2):G222–G231.
28. Grone HJ, Weber K, Helmchen U, et al. Villin—a marker of brush border differentiation and cellular origin in human renal cell carcinoma. *Am J Pathol.* 1986;124(2):294–302.
29. Alison MR, Guppy NJ, Lim SM, et al. Finding cancer stem cells: are aldehyde dehydrogenases fit for purpose? *J Pathol.* 2010;222(4):335–344.
30. Hirschmann-Jax C, Foster AE, Wulf GG, et al. A distinct "side population" of cells with high drug efflux capacity in human tumor cells. *Proc Natl Acad Sci U S A.* 2004;101(39):14228–14233.
31. Wang YH, Li F, Luo B, et al. A side population of cells from a human pancreatic carcinoma cell line harbors cancer stem cell characteristics. *Neoplasma.* 2009;56(5):371–378.
32. Larkin JM, Chowdhury S, Gore ME. Drug insight: advances in renal cell carcinoma and the role of targeted therapies. *Nat Clin Pract Oncol.* 2007; 4(8):470–479.
33. Monzani E, Facchetti F, Galmozzi E, et al. Melanoma contains CD133 and ABCG2 positive cells with enhanced tumourigenic potential. *Eur J Cancer.* 2007;43(5):935–946.
34. Morrison BJ, Schmidt CW, Lakhani SR, et al. Breast cancer stem cells: implications for therapy of breast cancer. *Breast Cancer Res.* 2008;10(4):210.
35. Collins AT, Berry PA, Hyde C, et al. Prospective identification of tumorigenic prostate cancer stem cells. *Cancer Res.* 2005;65(23):10946–10951.
36. McAllister SS, Weinberg RA. Tumor-host interactions: a far-reaching relationship. *J Clin Oncol.* 2010;28(26):4022–4028.
37. Eini H, Tejman-Yarden N, Lewis EC, et al. Association between renal injury and reduced interleukin-15 and interleukin-15 receptor levels in acute kidney injury. *J Interferon Cytokine Res.* 2010;30(1):1–8.
38. Eckardt KU, Bernhardt W, Willam C, et al. Hypoxia-inducible transcription factors and their role in renal disease. *Semin Nephrol.* 2007;27(3):363–372.
39. Srivastava VK, Nalbantoglu J. Flow cytometric characterization of the DAOY medulloblastoma cell line for the cancer stem-like phenotype. *Cytometry A.* 2008;73(10):940–948.
40. Waldmann TA. The biology of interleukin-2 and interleukin-15: implications for cancer therapy and vaccine design. *Nat Rev Immunol.* 2006;6(8): 595–601.
41. Arina A, Murillo O, Dubrot J, et al. Interleukin-15 liver gene transfer increases the number and function of IKDCs and NK cells. *Gene Ther.* 2008;15(7):473–483.
42. Meazza R, Lollini PL, Nanni P, et al. Gene transfer of a secretable form of IL-15 in murine adenocarcinoma cells: effects on tumorigenicity, metastatic potential and immune response. *Int J Cancer.* 2000;87(4):574–581.

43. Munger W, DeJoy SQ, Jeyaseelan R Sr, et al. Studies evaluating the antitumor activity and toxicity of interleukin-15, a new T cell growth factor: comparison with interleukin-2. *Cell Immunol.* 1995;165(2):289–293.
44. Waldmann TA, Lugli E, Roederer M, et al. Safety (toxicity), pharmacokinetics, immunogenicity, and impact on elements of the normal immune system of recombinant human IL-15 in rhesus macaques. *Blood.* 2011; 117(18):4787–4795.
45. Ogris M, Wagner E. To be targeted: is the magic bullet concept a viable option for synthetic nucleic acid therapeutics? *Hum Gene Ther.* 2011;22(7):799–807.
46. Munz C, Dao T, Ferlazzo G, et al. Mature myeloid dendritic cell subsets have distinct roles for activation and viability of circulating human natural killer cells. *Blood.* 2005;105(1):266–273.
47. Senju S, Matsunaga Y, Fukushima S, et al. Immunotherapy with pluripotent stem cell-derived dendritic cells [published online ahead of print April 5, 2011]. *Semin Immunopathol.* 2011.
48. Soleimani A, Berntsen A, Svane IM, et al. Immune responses in patients with metastatic renal cell carcinoma treated with dendritic cells pulsed with tumor lysate. *Scand J Immunol.* 2009;70(5):481–489.

Funding

This work was supported by grants from Agence de Biomédecine; ARC (Association pour la Recherche sur le Cancer) (RAC11005LLA); NRB-Vaincre le Cancer; Associazione Italiana per la Ricerca sul Cancro IG projects (5642 and 8912); and the Italian Ministry of Health. S.A. held doctoral fellowships from Société Française de Néphrologie, ARC, and NRB-Vaincre le Cancer. M.C. was supported by the Italian Neuroblastoma Foundation.

Notes

Study sponsors had no role in the design of the study; the collection, analysis, or interpretation of the data; the decision to submit the article for publication; or the writing of the article. The authors have no competing financial interests to declare.

Affiliations of authors: INSERM UMR 1014, Lavoisier Building, Paul Brousse Hospital, Villejuif, France (SA, JG-M, AD, AV, BC, BA, PE); Université de Paris Sud XI, Le Kremlin-Bicêtre France (SA, JG-M, DC, AD, AV, BC, BA, PE); Molecular Biotechnology Center and Department of Internal Medicine, University of Turin, Turin, Italy (SB, GC); Laboratory of Immunotherapy, National Cancer Research Institute, Genoa, Italy (MC, SF); INSERM UMR 753, Institut Gustave Roussy (IGR), Villejuif, France (SC); INSERM UMR 972, Paul Brousse Hospital, Villejuif, France (DC).